Anal. Chem. **2010,** *82,* 7656–7659

Visualizing Resonances in the Complex Plane with Vibrational Phase Contrast Coherent Anti-Stokes Raman Scattering

Martin Jurna,[†] Erik T. Garbacik,[†] Jeroen P. Korterik,[†] Jennifer L. Herek,[†] Cees Otto,[‡] and Herman L. Offerhaus*,[†]

Optical Sciences, MESA+ Institute for Nanotechnology, University of Twente, Enschede, The Netherlands, and Medical Cell BioPhysics, MIRA Institute for Biomedical Technology and Technical Medicine, University of Twente, Enschede, The Netherlands

In coherent anti-Stokes Raman scattering (CARS), the emitted signal carries both amplitude and phase information of the molecules in the focal volume. Most CARS experiments ignore the phase component, but its detection allows for two advantages over intensity-only CARS. First, the pure resonant response can be determined, and the nonresonant background rejected, by extracting the imaginary component of the complex response, enhancing the sensitivity of CARS measurements. Second, selectivity is increased via determination of the phase and amplitude, allowing separation of individual molecular components of a sample even when their vibrational bands overlap. Here, using vibrational phase contrast CARS (VPC-CARS), we demonstrate enhanced sensitivity in quantitative measurements of ethanol/methanol mixtures and increased selectivity in a heterogeneous mixture of plastics and water. This powerful technique opens a wide range of possibilities for studies of complicated systems where overlapping resonances limit standard methodologies.

As the field of coherent anti-Stokes Raman scattering (CARS) has advanced, the challenge of probing ever-smaller concentrations of resonant molecules has driven the development of techniques that reduce or remove the nonresonant background that complicates CARS experiments. Established approaches work in a variety of ways: exploiting the polarization differences in resonant and nonresonant responses,[1,2] measuring phase delays relative to a stable local oscillator,[3,4] utilizing broadband spectral phase shaping,[5−8] enhancing contrast based on differences in the dephasing times of resonant and nonresonant intermediate states,[9] or some combination thereof.[10] These techniques can be used to analyze samples in which overlapping vibrational bands are not an issue, but biological systems can have many molecules with very similar vibrational spectra. In these cases, measuring only the amplitude of the resonant CARS response is insufficient to distinguish between species.

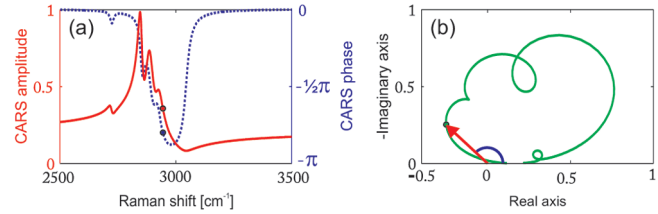

Figure 1. Complementary depictions of driven, damped resonances. (a) Amplitude (red) and phase (blue) of the resonances of bulk polyethylene around 3000 cm^{-1}. (b) Complex plane representation of the polyethylene resonances.

For a given driving frequency, the anti-Stokes emission of a molecule in the focal volume will have an amplitude and phase relative to the input fields that can be represented as a point in the complex plane defined by a vector length and angle, as shown in Figure 1. A single isolated resonance traces a circle in the complex plane as a function of frequency, while multiple resonances result in additional loops. The offset of the trajectory on the real axis corresponds to the nonresonant background. The imaginary component relates to the background-free resonant Raman response, while the real component contains information about both the resonant and the nonresonant components of the $\chi^{(3)}$ tensor.[11]

The general solution to a damped, driven harmonic oscillator is a complex Lorentzian, which has a phase that will range from 0 to $-\pi$ as the driving frequency is increased through a vibrational resonance. As such, the imaginary component of the complex

* To whom correspondence should be addressed. E-mail: h.l.offerhaus@tnw.utwente.nl.

† Optical Sciences, MESA+ Institute for Nanotechnology.

‡ Medical Cell BioPhysics, MIRA Institute for Biomedical Technology and Technical Medicine.

(1) Chikishev, A.; Lucassen, G.; Koroteev, N.; Otto, C.; Greve, J. *Biophys. J.* **1992**, *63*, 976–985.
(2) Cheng, J.-X.; Book, L. D.; Xie, X. S. *Opt. Lett.* **2001**, *26*, 1341–1343.
(3) Potma, E. O.; Evans, C. L.; Xie, X. S. *Opt. Lett.* **2006**, *31*, 241–243.
(4) Jurna, M.; Korterik, J. P.; Otto, C.; Offerhaus, H. L. *Opt. Express* **2007**, *15*, 15207–15213.
(5) Oron, D.; Dudovich, N.; Yelin, D.; Silberberg, Y. *Phys. Rev. A* **2002**, *65*, 043408.
(6) Scully, M. O.; Kattawar, G. W.; Lucht, R. P.; Opatrny, T.; Pilloff, H.; Rebane, A.; Sokolov, A. V.; Zubairy, M. S. *Proc. Natl. Acad. Sci. U.S.A.* **2002**, *99*, 10994–11001.
(7) Hellerer, T.; Enejder, A. M. K.; Zumbusch, A. *Appl. Phys. Lett.* **2004**, *85*, 25–27.
(8) van Rhijn, A. C. W.; Offerhaus, H. L.; van der Walle, P.; Herek, J. L.; Jafarpour, A. *Opt. Express* **2010**, *18*, 2695–2709.
(9) Volkmer, A.; Book, L. D.; Xie, X. S. *Appl. Phys. Lett.* **2002**, *80*, 1505–1507.
(10) Orsel, K.; Garbacik, E. T.; Jurna, M.; Korterik, J. P.; Otto, C.; Herek, J. L.; Offerhaus, H. L. *J. Raman Spectrosc.* **2010**, DOI: 10.1002/jrs.2621.
(11) Lucassen, G. Ph. D. Thesis, University of Twente, Enschede, the Netherlands, 1992.

10.1021/ac101453s
Published on Web 08/23/2010

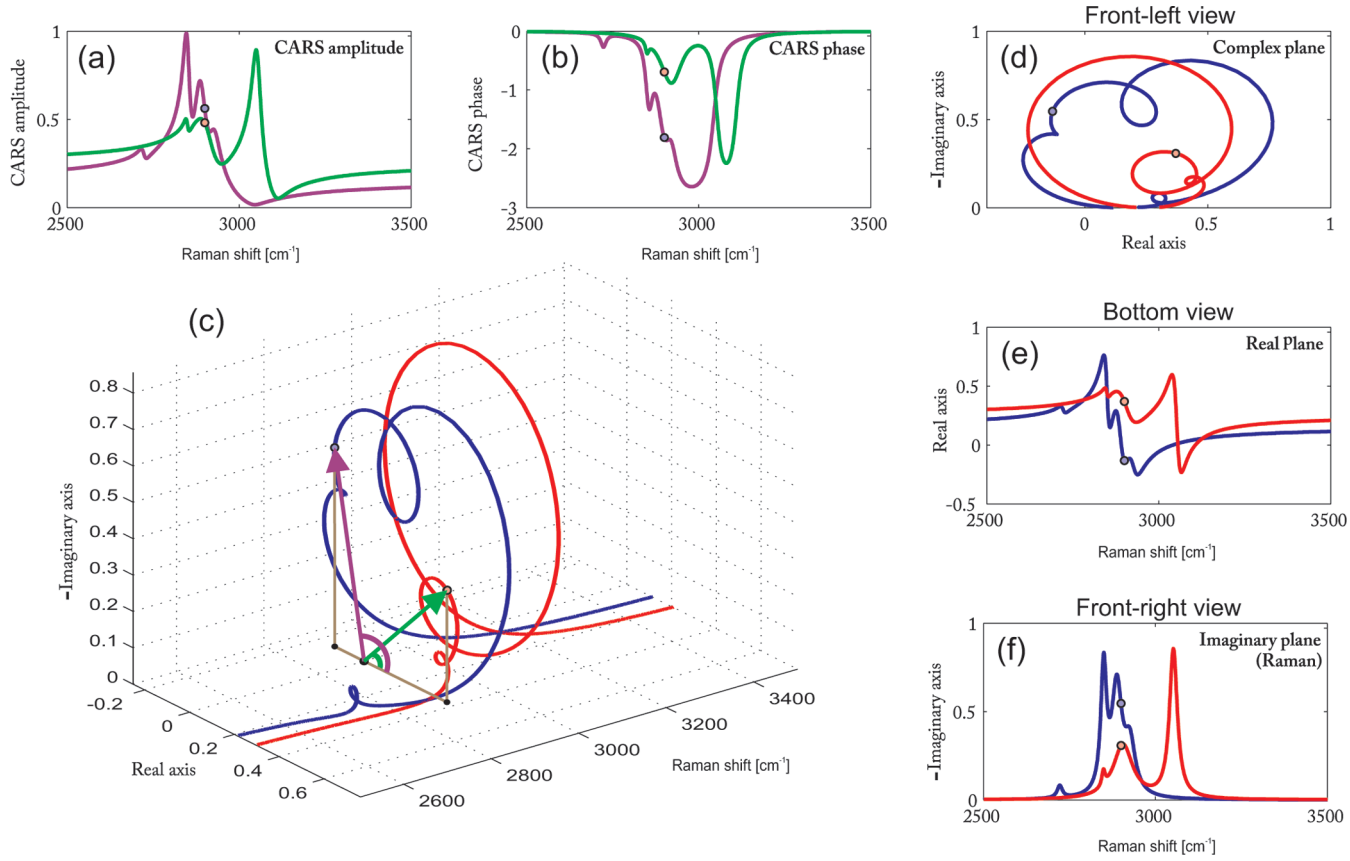

Figure 2. The trajectories of the vibrational responses of polyethylene and polystyrene through complex space near 3000 cm^{-1}. The amplitudes (a) and phases (b) of the CARS responses of these two plastics are shown in violet and green, respectively. When the amplitude and phase are plotted against the driving frequency, the spirals in part c are constructed. Projections along each axis of this 3-D space are shown on the right side and correspond to the full complex trajectory (d, projection along frequency axis), the real component of the complex response as a function of frequency (e, projection along imaginary axis), and the background-free Raman spectrum (f, projection along real axis). The blue and red dots in each figure correspond to the locations of polyethylene and polystyrene at 2900 cm^{-1}, respectively.

trajectory will always have a negative value. To maintain consistency with the convention of Raman scattering as a positive quantity, we plot the complex plane mirrored across the real axis by inverting the sign of the imaginary component.

The added value of the complex plane representation is most apparent when two or more chemical species with overlapping vibrational bands are present, as illustrated in Figure 2a for two common plastics. At 2900 cm^{-1}, the CARS amplitudes of polyethylene and polystyrene are very similar, but their phases are well separated, shown in Figure 2b. Plotting the amplitude and phase of each material against the driving frequency constructs a spiral or corkscrew pattern in complex space, as illustrated in Figure. 2c. The projection along the frequency axis (Figure 2d) shows the complex plane; along the imaginary axis (Figure 2e) shows the real component, with the typical dispersion caused by wavelength-dependent refractive index changes; and along the real axis (Figure 2f), the imaginary component is shown, with the resonant (Raman) part of the response. Being able to probe both the phase and amplitude of a sample simultaneously increases the chemical selectivity. The main advantage of this visualization is the ease with which the appropriate driving frequency can be determined to maximize separation of the two components in complex space, thereby optimizing chemical selectivity.

We recently reported a technique called vibrational phase contrast CARS (VPC-CARS) whereby the vibrational phase of the scatterers in a sample can be determined directly via two interfering CARS pathways.[12] When the focal volume contains only one type of molecule, we obtain points in the complex plane as shown in (I) and (III) in Figure 3. A single measurement on a mixed sample yields the combination of all of the amplitudes and phases of the molecules in the focal volume; the signal from these molecules is added coherently. A mixture of molecules that interact weakly, e.g., via London dispersion forces, will result in linear combinations of the individual molecular amplitudes and phases proportional to

$$A_m\, e^{-i\phi_m} \propto N_{(I)}A_{(I)}(\Omega)\, e^{-i\phi_{(I)}(\Omega)} + N_{(III)}A_{(III)}(\Omega)\, e^{-i\phi_{(III)}(\Omega)} \quad (1)$$

where Ω is the driving frequency, N_n is the molar concentration of each compound, and A_n and ϕ_n are the amplitude and phase, respectively, of the response of each individual species. For example, a 1/1 molar mixture of the two types of molecules (I) and (III) will result in the complex vector sum (II) in Figure

(12) Jurna, M.; Korterik, J. P.; Otto, C.; Herek, J. L.; Offerhaus, H. L. *Phys. Rev. Lett.* **2009**, *103*, 043905-1–043905-3.

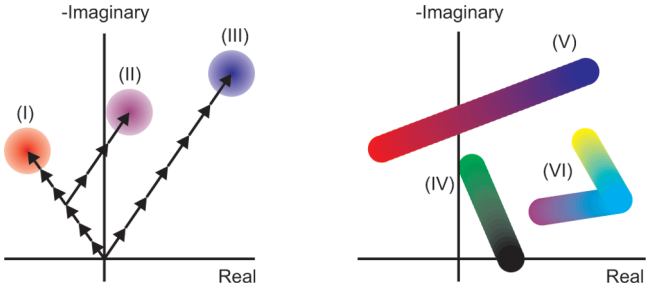

Figure 3. Complex plane vectors at a single driving frequency. Left: compounds (I) and (III) contain the same number of molecules but have different phase angles and amplitudes. A 1/1 molar mixture of compounds (I) and (III) gives location (II) in the complex plane. Right: (IV) shows the dilution of a resonant compound in a nonresonant compound, (V) shows a mixing between two resonant compounds, and (VI) shows a chemical reaction between two resonant species yielding a resonant product.

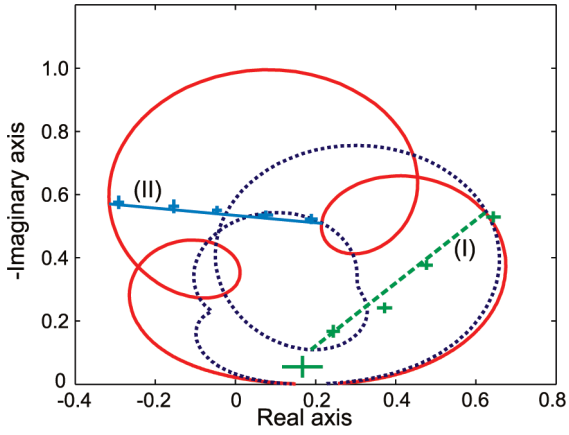

Figure 4. Complex plane representations of pure ethanol (red, solid) and methanol (purple, dotted). The straight lines represent the predicted dissolution trajectories of ethanol/methanol mixtures at 2871 cm^{-1} (I, green, dashed) and 2937 cm^{-1} (II, blue, solid), while the crosses are measured data points at mixing ratios of 100/0, 75/25, 50/50, 25/75, and 0/100. The right end of line (I) terminates on the red curve, while the right end of line (II) ends on the purple curve. The bars on each data point indicate the measurement error.

3. By extension, any stoichiometric mixture of compounds (I) and (III) will fall on the line connecting points (I) and (III) in the complex plane. If one of the two compounds is not resonant at the driving frequency, then its phase $\phi \rightarrow 0$, and its complex vector will lie on the real axis.

When a resonant solute is mixed with a nonresonant solvent, we expect the trajectory shown in Figure 3 as trajectory (IV). Two weakly interacting resonant compounds mixed together will produce Figure 3 trajectory (V). Other systems that can produce trajectory (V) include molecular conformational changes where an intramolecular rearrangement results in changes in the vibrational frequencies of the individual covalent bonds or a material phase transition such as crystallization, wherein modified intermolecular forces generate amplitude and/or phase differences between the starting and ending material phases. The chemical reaction of two resonant reactants into a resonant product can result in a trajectory like that of Figure 3 trajectory (VI).

As an example of Figure 3 trajectory (V), the calculated trajectories of ethanol and methanol are shown in Figure 4, based on Raman spectra of the pure substances. Experimental results

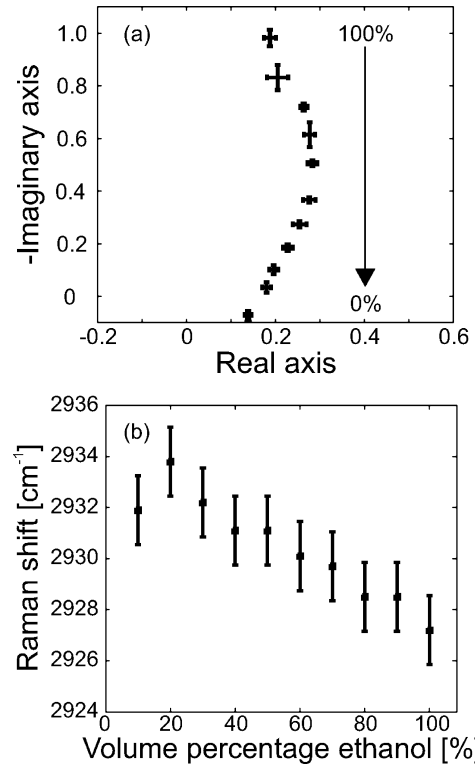

Figure 5. Dilution of ethanol in water as function of volume percentage. The deviation from a straight mixing trajectory (a) is caused by a shift of the ethanol Raman peak at 2937 cm^{-1} (b) due to strong interactions between the two compounds.

of ethanol/methanol mixtures were produced at five concentrations, from pure ethanol to pure methanol with 25% volume percentage mixing steps. The calculated trajectories of the linear mixtures of the two pure compounds at two different driving frequencies are shown as straight lines in Figure 4, while crosses indicate measured data points, with error bars of 1 standard deviation. The mixtures were measured at 2871 and 2937 cm^{-1}, yielding the green and blue lines in Figure 4, respectively.

When two compounds in a mixture interact strongly, e.g., through hydrogen bonding, the Raman peaks of those two compounds shift and the trajectory in the complex plane deviates from a straight line. An example of this effect is shown in Figure 5. The plot in Figure 5a was obtained at 2927 cm^{-1} for different mixing ratios of resonant ethanol with nonresonant water. A total of 11 samples were measured, ranging from pure ethanol to pure water with 10% volume ratio intervals. The curvature in Figure 5a is consistent with spontaneous Raman scattering data on the location of the resonance peak of ethanol as a function of the mixing ratio with water, shown in Figure 5b. The peak at 2927 cm^{-1} shifts toward higher Raman frequencies when the ethanol is diluted with water and is accompanied by a shift of the associated vibrational phase. The mixing dynamics of strongly interacting compounds therefore cannot be simply modeled as linear combinations of the complex vectors of the individual species.

In complicated samples that include more than two substances, the differences in amplitude between the various compounds can be very small but the difference in phase can be substantial. To demonstrate the imaging selectivity of our technique, a heterogeneous mixture of three different materials was imaged with

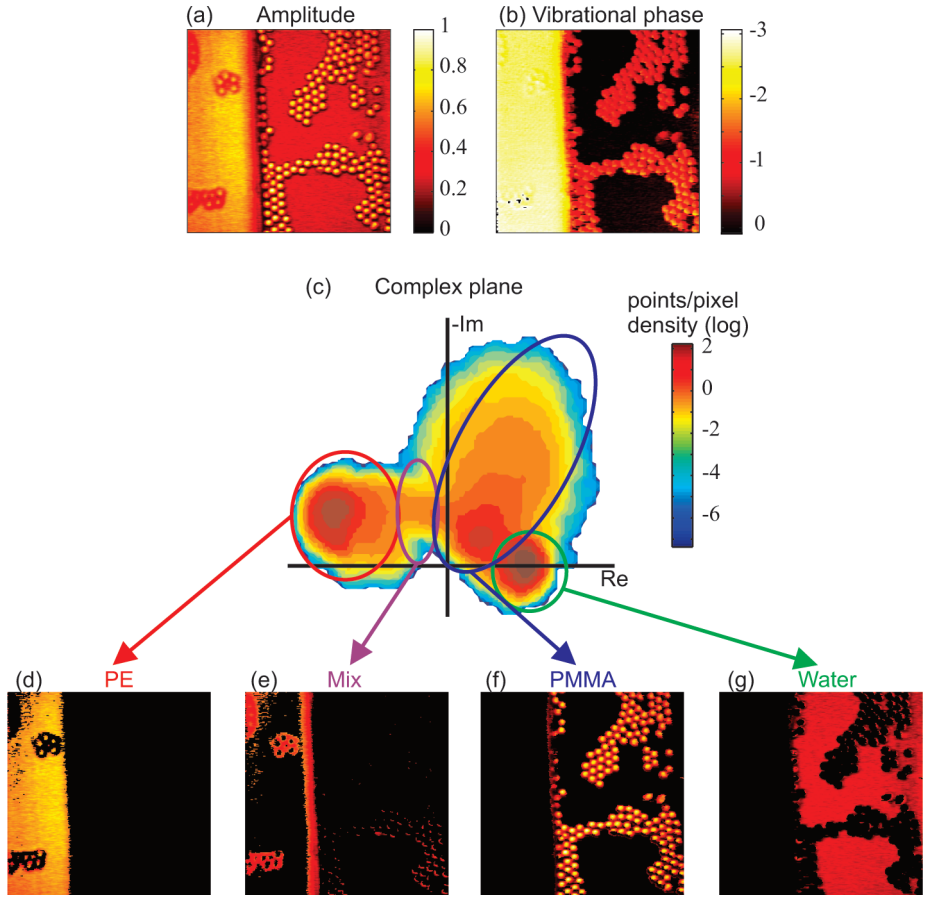

Figure 6. Measurement of the amplitude and phase at each location in a sample allows identification of the individual components. Top: amplitude (a) and vibrational phase (b) of a sample containing a sheet of PE, 4 μm PMMA beads, and water, imaged at 2940 cm^{-1}. Middle: density graph of the projected amplitude and vibrational phase points in the complex plane (c). Bottom: multicomponent analysis, where the different components (d−g) are separated by their location in the complex plane. The "mix" plot shows regions of the image where all three components are represented in the same focal volume. Each image is 100 μm × 100 μm.

VPC-CARS at a frequency of 2940 cm^{-1}, displayed in Figure 6. The sample contains a PE sheet, 4 μm poly(methyl)-methacrylate (PMMA) beads, and water. The amplitudes (Figure 6a) of all three materials are very similar at this frequency. However, the phase image (Figure 6b) presents a clear difference between the water, which is nonresonant, and the PE and PMMA. When the amplitude and phase information of all points in the image are displayed as a density plot in the complex plane, multiple distinct regions emerge. The points in these regions can be used to locate the three pure constituents. Between the PE, the PMMA, and the water there is a crossing area, showing the points where the focal volume consists of a mix of compounds. The reconstructed images shown in Figure 6e−h from the density complex plane are all free from background signal; they relate only to the (complex) signal from the substances. This example illustrates how VPC-CARS allows for multicomponent separation at a single vibrational resonance.

Vibrational phase contrast CARS is a powerful technique for increasing both the sensitivity and selectivity of vibrational imaging, with a wide range of possible applications. Accurate quantitative measurements of homogeneous mixtures can be made even when the amplitudes of the individual components are similar and can be extended to mixtures of more than two components. Chemical selectivity within complicated heterogeneous mixtures is straightforward through identification of regions of the complex plane corresponding to each individual compound. The extra dimension provided by direct measurement of the phase could grant insights into a wide range of scientific questions, such as the temporal dynamics of chemical reactions or the behavior of cells during replication.

ACKNOWLEDGMENT

M.J. and E.T.G. contributed equally to this work. Funding for this research is provided by NanoNed, a nanotechnology program of the Dutch Ministry of Economic Affairs, and by the Stichting voor Fundamenteel Onderzoek der Materie (FOM), which is financially supported by the Nederlandse Organisatie voor Wetenschappelijk Onderzoek (NWO). We acknowledge Coherent Inc. for the use of a Paladin laser and APE Berlin for the collaboration and use of a Levante Emerald OPO. Furthermore, we would like to thank K. Orsel for the spontaneous Raman spectra of ethanol and methanol and A.C.W. van Rhijn and B. Lansdorp for useful discussions.

Received for review June 2, 2010. Accepted August 2, 2010.

AC101453S